

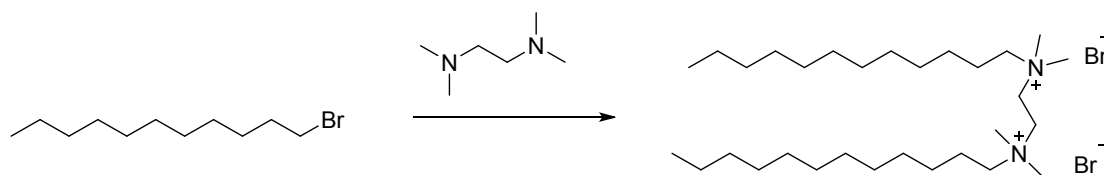
Highly stable foams generated in mixed systems of ethanediyl-1, 2-bis(dodecyldimethylammonium bromide) and alcohols

Bing-Lei Song¹, Xiao-Na Yu¹, Jian-Xi Zhao^{2*}, Guo-Jing Sun²

1. The Key Laboratory of Food Colloids and Biotechnology, Ministry of Education, School of Chemical and Material Engineering, Jiangnan University, Wuxi, Jiangsu 214122, P. R. China

2. Institute of Colloid and Interface Chemistry, College of Chemistry and Chemical Engineering, Fuzhou University, Fuzhou, Fujian, 350108, P. R. China

1. Synthesis of ethanediyl-1, 2-bis(dodecyldimethylammonium bromide) (12-2-12)



Scheme S1 The synthetic procedure of 12-2-12

1-Bromododecane (30g, 0.12mol), N,N,N',N'-tetramethylethylenediamine (5.8g, 0.05mol) and 100mL ethanol were added into a flask equipped with a reflux condenser. The reaction was carried out at 85°C for 24h. The solvent in the reaction mixture was removed under reduced pressure. The remaining solid was recrystallized with ethanol/ethyl acetate twice. After dried under vacuum at 45 °C, the final product was obtained as white powder. Yield: 41.3%.

¹H NMR (400 MHz, CDCl₃) δ 4.64 (s, 4H), 3.64 (t, *J* = 7.8 Hz, 4H), 3.44 (s, 12H), 1.75 (s, 4H), 1.31-1.19 (m, 36H), 0.81 (t, *J* = 6.8 Hz, 6H).

Elemental analysis

Anal. Calcd. for C₃₀H₆₆Br₂N₂: C, 58.62; H, 10.82; N, 4.56. Found: C, 58.39; H, 11.01; N, 4.45.

2. The interfacial dilational experiment data and fitting results with LVT model of different systems

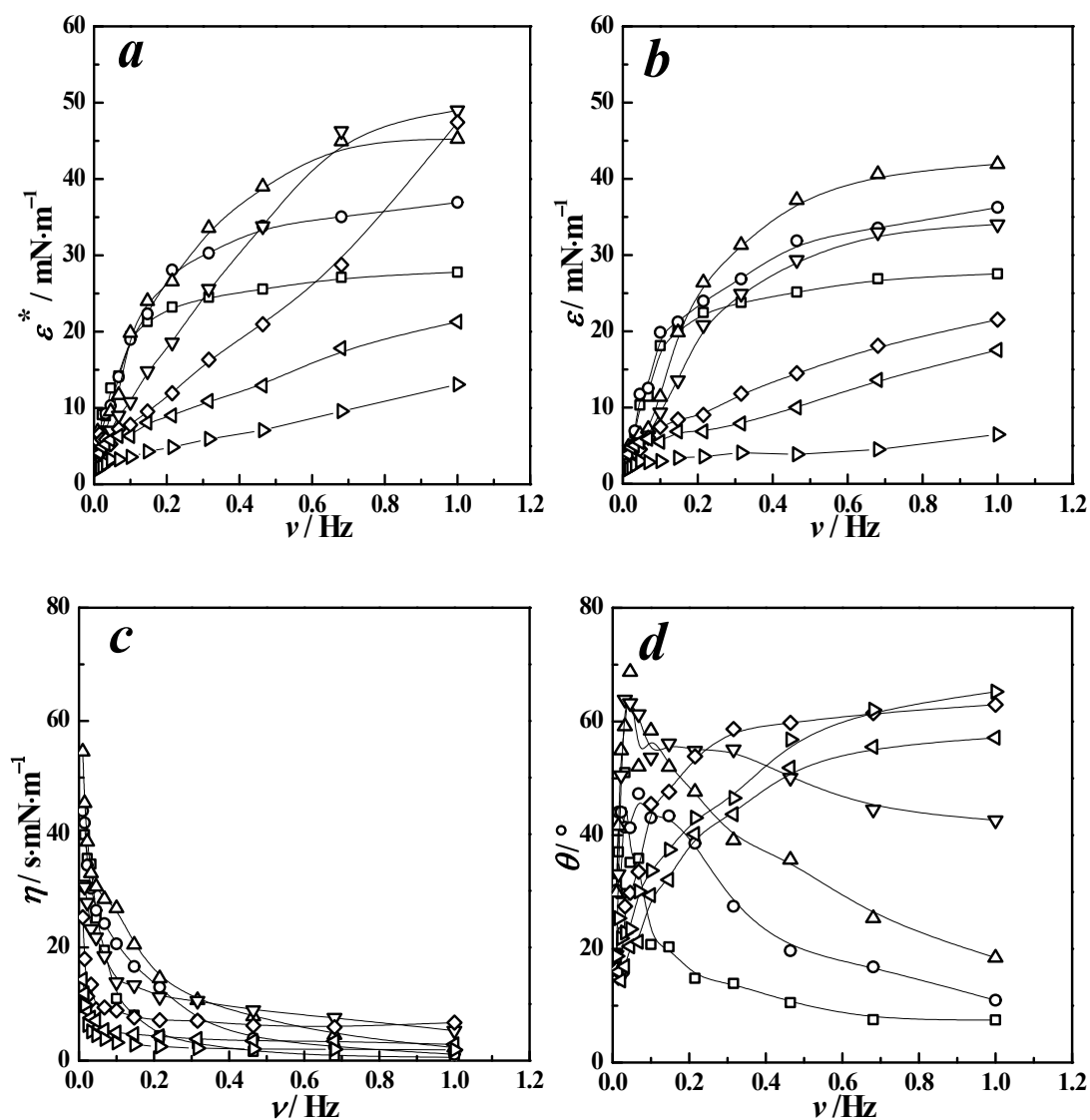


Fig.S1 The experimental plots of complex modulus (ϵ^* , *a*), interfacial elasticity (ϵ , *b*), interfacial viscosity (η , *c*) and phase angle (θ , *d*), as a function of frequency (ν), respectively, in 12-2-12/5.5mMC₆OH aqueous solutions at 25°C. The symbols represent different surfactant concentrations: $\log(C/\text{mmol}\cdot\text{L}^{-1}) = -1.38$ (\square), -1.18 (\circ), -1.00 (\triangle), -0.78 (∇), -0.60 (\diamond), -0.40 (\triangleleft), 0.20 (χ).

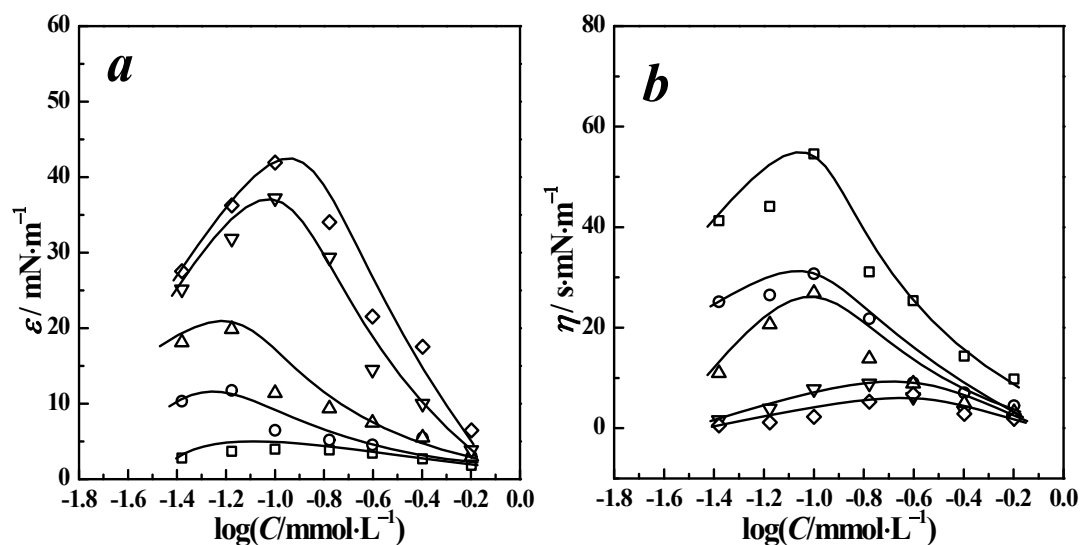


Fig.S2 Semilogarithmic plots of dilational interfacial elasticity (ϵ , *a*) and interfacial viscosity (η , *b*) of 12-2-12/5.5mMC₆OH as a function of the surfactant concentration C for different frequencies.

The symbols represent $\nu/\text{Hz} = 0.010$ (\square), 0.046 (\circ), 0.100 (\triangle), 0.464 (∇) and 1.000 (\diamond)

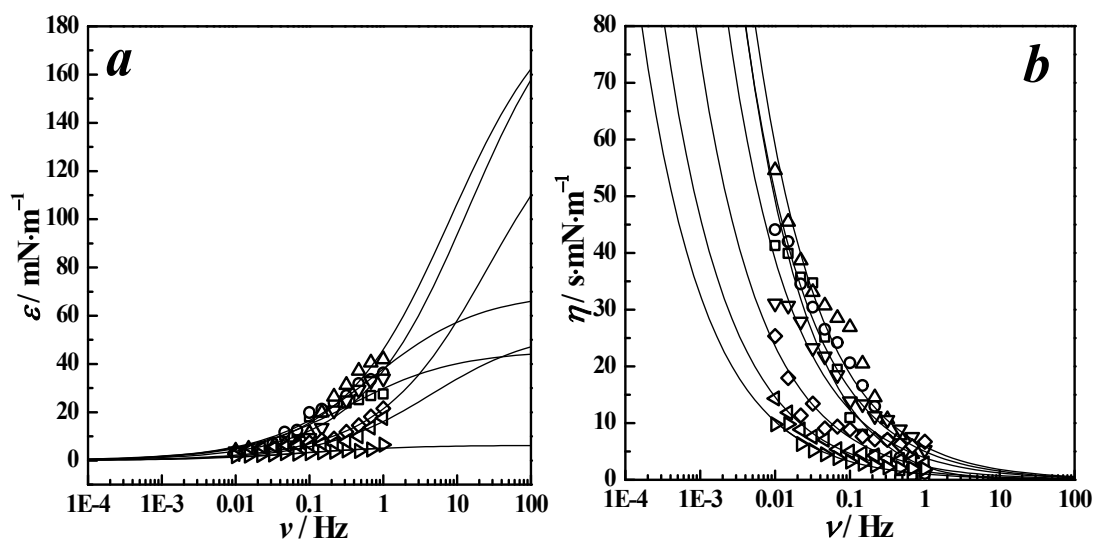


Fig.S3 Fitting results of dilational interfacial elasticity (ϵ , *a*) and interfacial viscosity (η , *b*) in terms of LVT model for 12-2-12/5.5mMC₆OH aqueous solutions at 25°C. The symbols represent different surfactant concentrations: $\log(C/\text{mmole}\cdot\text{L}^{-1}) = -1.38$ (\square), -1.18 (\circ), -1.00 (\triangle), -0.78 (∇), -0.60 (\diamond), -0.40 (\triangleleft), 0.20 (χ).

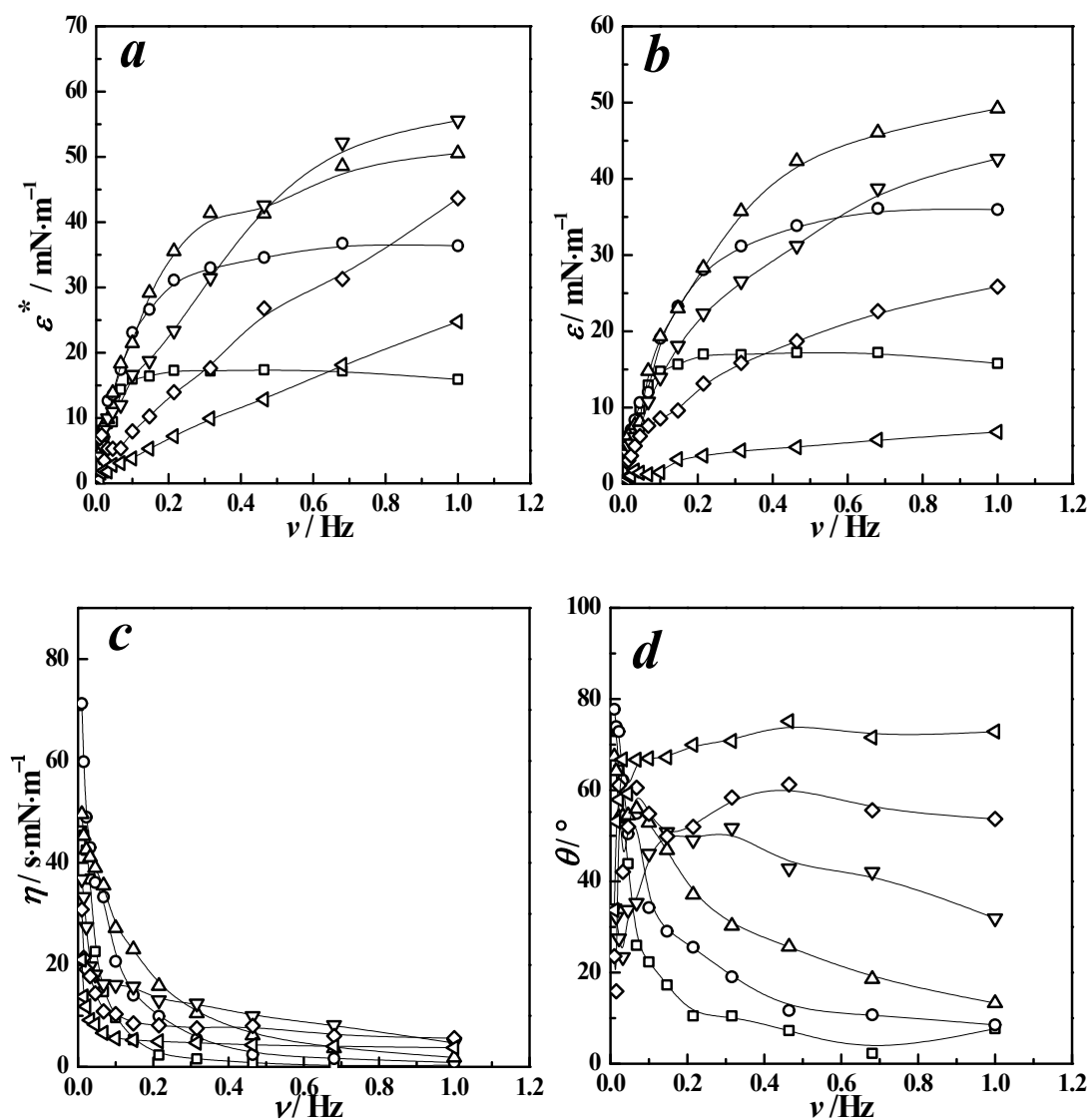


Fig.S4 The experimental plots of complex modulus (ϵ^* , *a*), interfacial elasticity (ϵ , *b*), interfacial viscosity (η , *c*) and phase angle (θ , *d*), as a function of frequency (ν), respectively, in 12-2-12/4mMC₆OH aqueous solutions at 25°C. The symbols represent different surfactant concentrations: $\log(C/\text{mmol}\cdot\text{L}^{-1}) = -1.38$ (□), -1.18 (○), -1.00 (△), -0.78 (▽), -0.60 (◇), -0.40 (<)

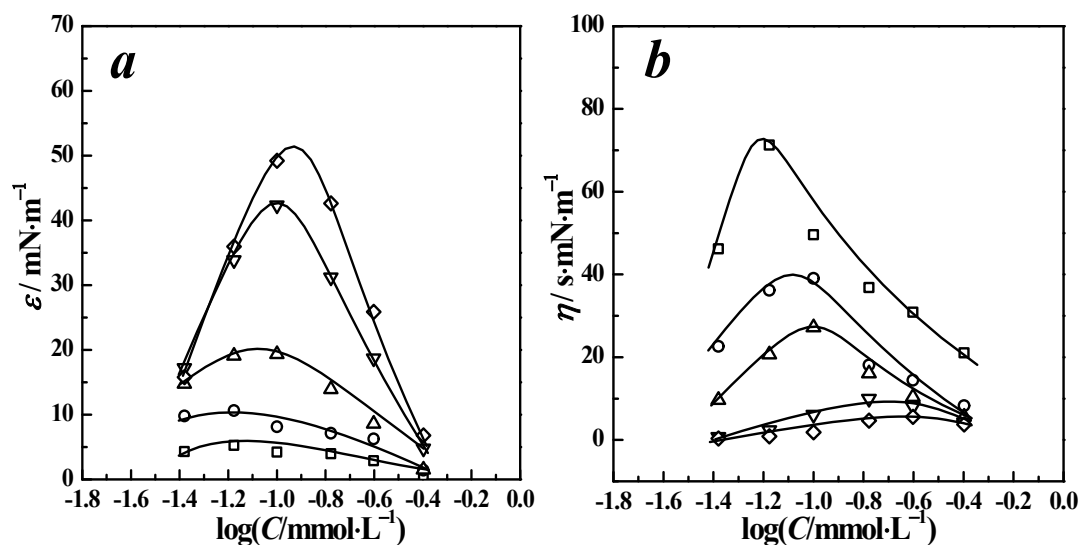


Fig.S5 Semilogarithmic plots of dilational interfacial elasticity (ϵ , *a*) and interfacial viscosity (η , *b*) of 12-2-12/4mMC₆OH as a function of the surfactant concentration C for different frequencies. The symbols represent $\nu/\text{Hz} = 0.010$ (\square), 0.046 (\circ), 0.100 (\triangle), 0.464 (∇) and 1.000 (\diamond)

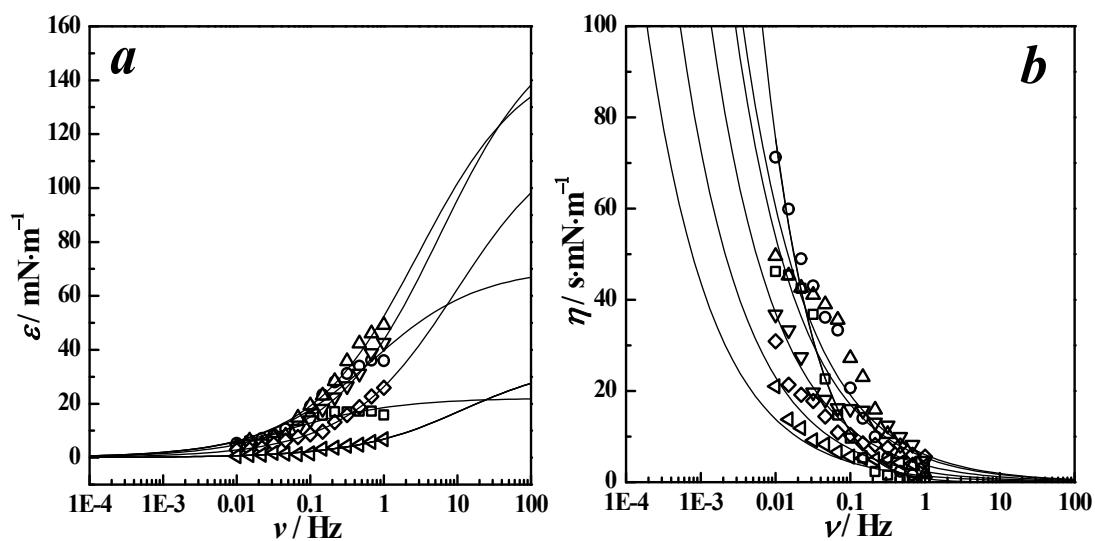


Fig.S6 Fitting results of dilational interfacial elasticity (ϵ , *a*) and interfacial viscosity (η , *b*) in terms of LVT model for 12-2-12/4mMC₆OH aqueous solutions at 25°C. The symbols represent different surfactant concentrations: $\log(C/\text{mmole}\cdot\text{L}^{-1}) = -1.38$ (\square), -1.18 (\circ), -1.00 (\triangle), -0.78 (∇), -0.60 (\diamond), -0.40 (\triangleleft)

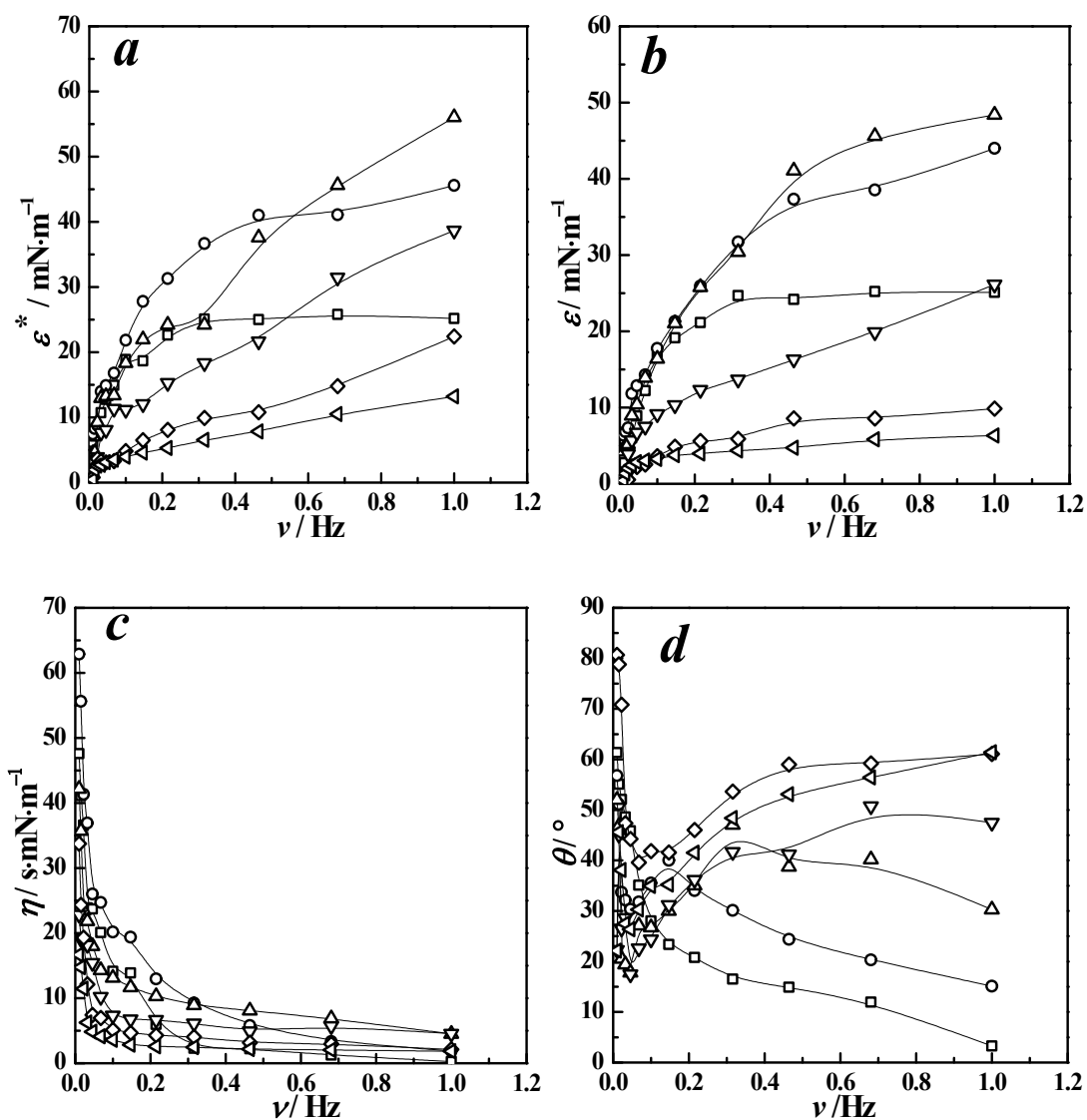


Fig.S7 The experimental plots of complex modulus (ϵ^* , *a*), interfacial elasticity (ϵ , *b*), interfacial viscosity (η , *c*) and phase angle (θ , *d*), as a function of frequency (ν), respectively, in 12-2-12/8mMC₆OH aqueous solutions at 25°C. The symbols represent different surfactant concentrations: $\log(C/\text{mmol}\cdot\text{L}^{-1}) = -1.38$ (□), -1.00 (○), -0.78 (△), -0.60 (▽), -0.40 (◇), -0.20 (<)

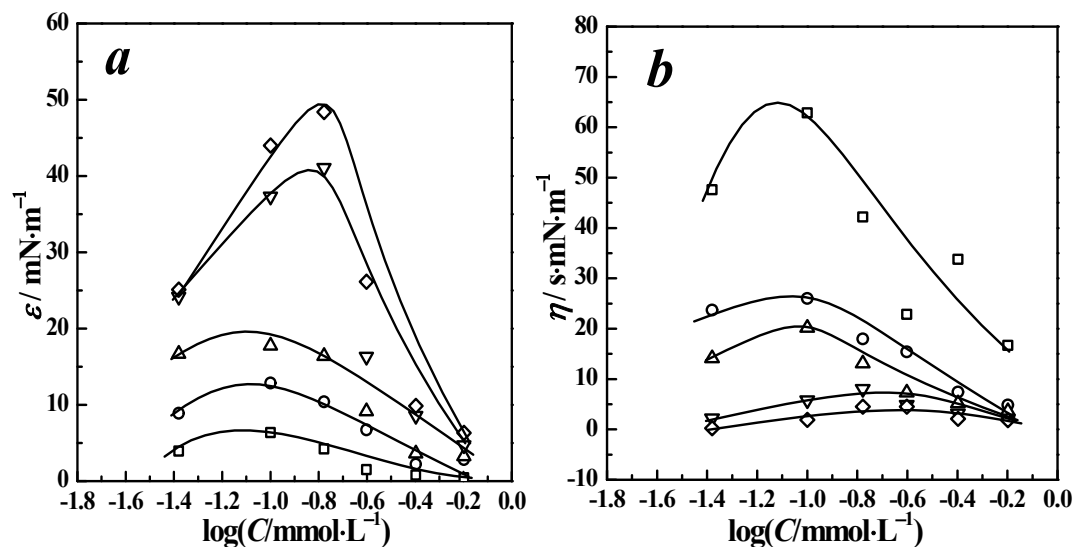


Fig.S8 Semilogarithmic plots of dilational interfacial elasticity (ϵ , *a*) and interfacial viscosity (η , *b*) of 12-2-12/8mMC₆OH as a function of the surfactant concentration C for different frequencies. The symbols represent $\nu/\text{Hz} = 0.010$ (\square), 0.046 (\circ), 0.100 (\triangle), 0.464 (∇) and 1.000 (\diamond)

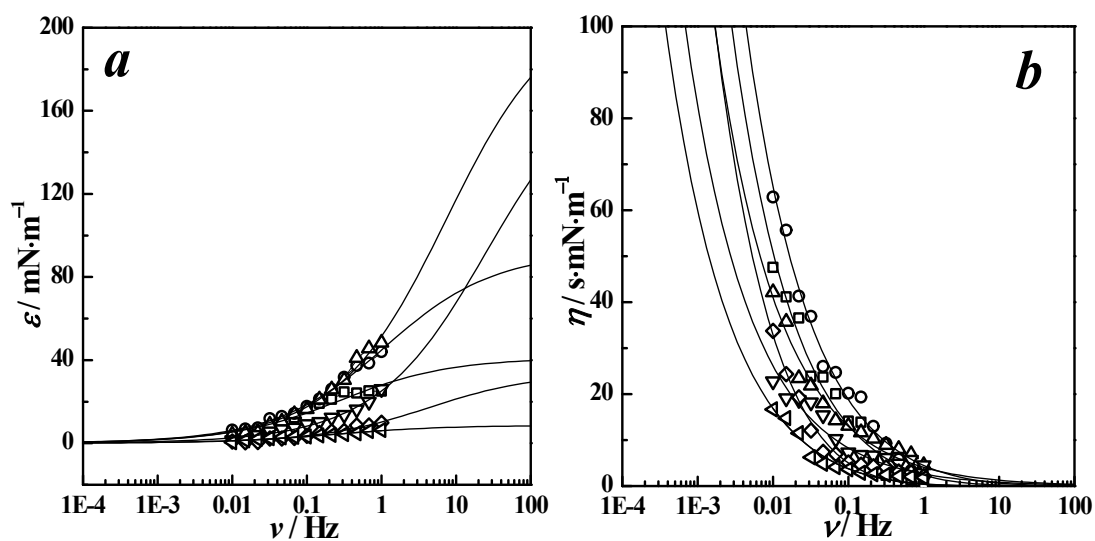


Fig.S9 Fitting results of dilational interfacial elasticity (ϵ , *a*) and interfacial viscosity (η , *b*) in terms of LVT model for 12-2-12/8mMC₆OH aqueous solutions at 25°C. The symbols represent different surfactant concentrations: $\log(C/\text{mmol}\cdot\text{L}^{-1}) = -1.38$ (\square), -1.00 (\circ), -0.78 (\triangle), -0.60 (∇), -0.40 (\diamond), -0.20 ($<$)

Table S1 Foam decay time $t_{1/2}^{\max}$ and limiting interfacial elasticity $\varepsilon_{0,fit}$ of 12-2-12/4mMC₆OH, 12-2-12/5.5mMC₆OH and 12-2-12/8mMC₆OH mixed systems at the surface excess of 80%

system	12-2-12/4mMC ₆ OH	12-2-12/5.5mMC ₆ OH	12-2-12/8mMC ₆ OH
$10^{10}\Gamma_{\max}$ mol·cm ⁻²	3.62	3.98	2.46
80%* $10^{10}\Gamma_{\max}$ /mol·cm ⁻²	2.90	3.18	1.97
C/mmol·L ⁻¹	0.057	0.036	0.076
$\varepsilon_{0,fit}$ /mN·m ⁻¹	54.17	66.33	56.67
$t_{1/2}^{\max}$ /min	958	1413	1188

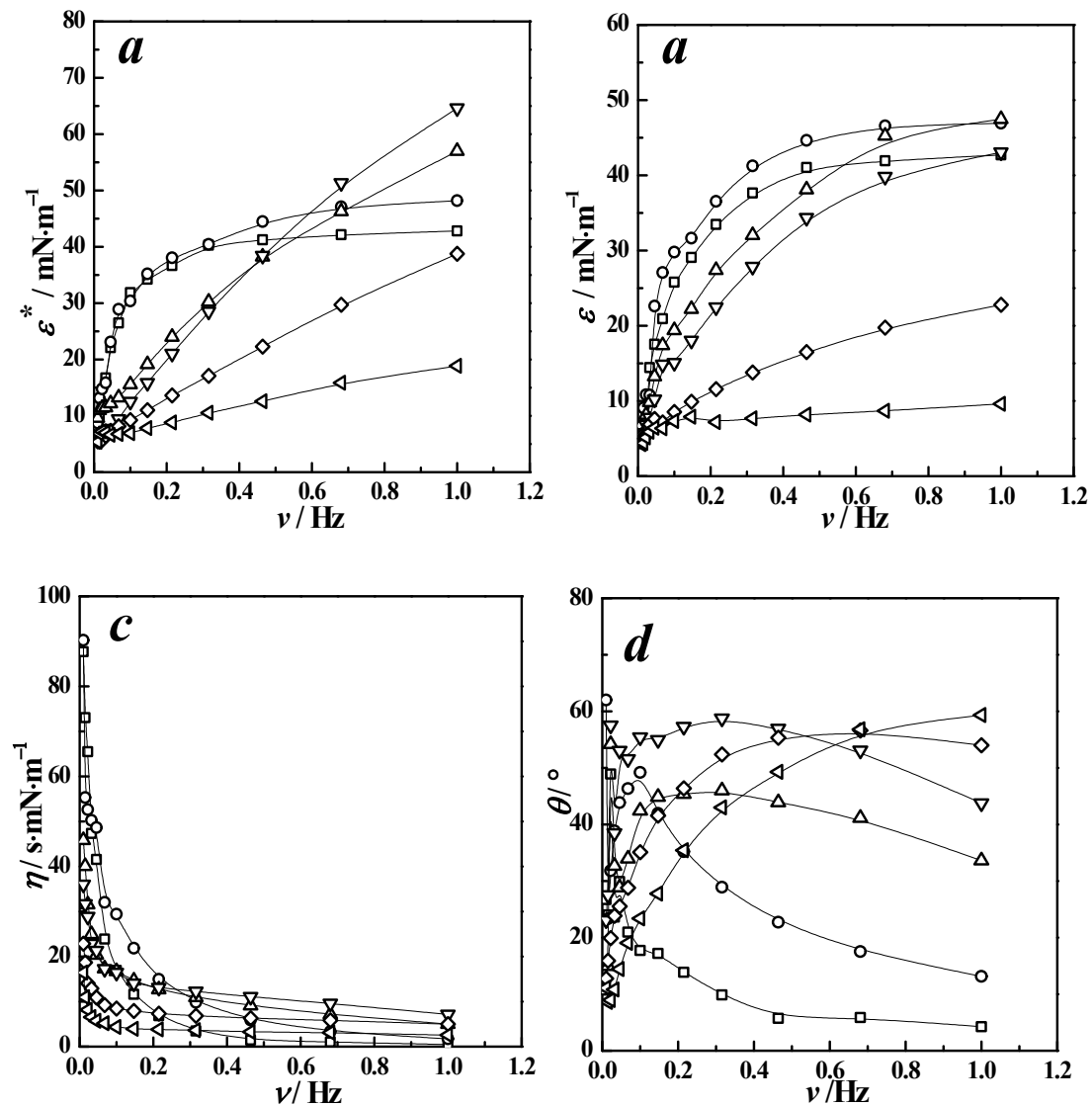


Fig.S10 The experimental plots of complex modulus (ε^* , a), interfacial elasticity (ε , b), interfacial

viscosity (η , c) and phase angle (θ , d), as a function of frequency (ν), respectively, in 12-2-12/0.3mMC₇OH aqueous solutions at 25°C. The symbols represent different surfactant concentrations: $\log(C/\text{mmol}\cdot\text{L}^{-1}) = -1.30$ (\square), -1.18 (\circ), -0.93 (\triangle), -0.74 (∇), -0.52 (\diamond), -0.30 (\blacktriangleleft)

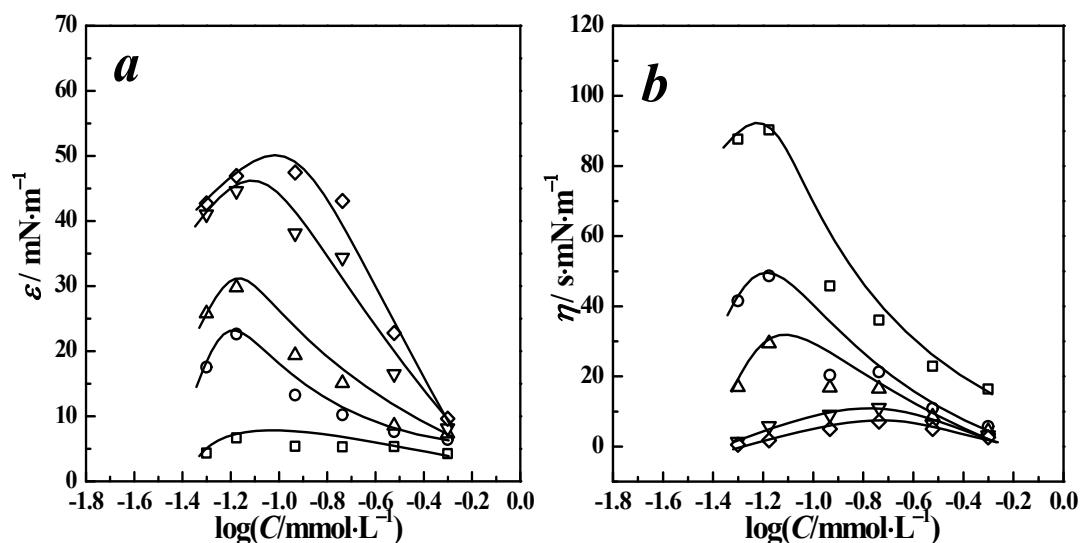


Fig.S11 Semilogarithmic plots of dilational interfacial elasticity (ϵ , a) and interfacial viscosity (η , b) of 12-2-12/0.3mMC₇OH as a function of the surfactant concentration C for different frequencies. The symbols represent $\nu/\text{Hz} = 0.010$ (\square), 0.046 (\circ), 0.100 (\triangle), 0.464 (∇) and 1.000 (\diamond)

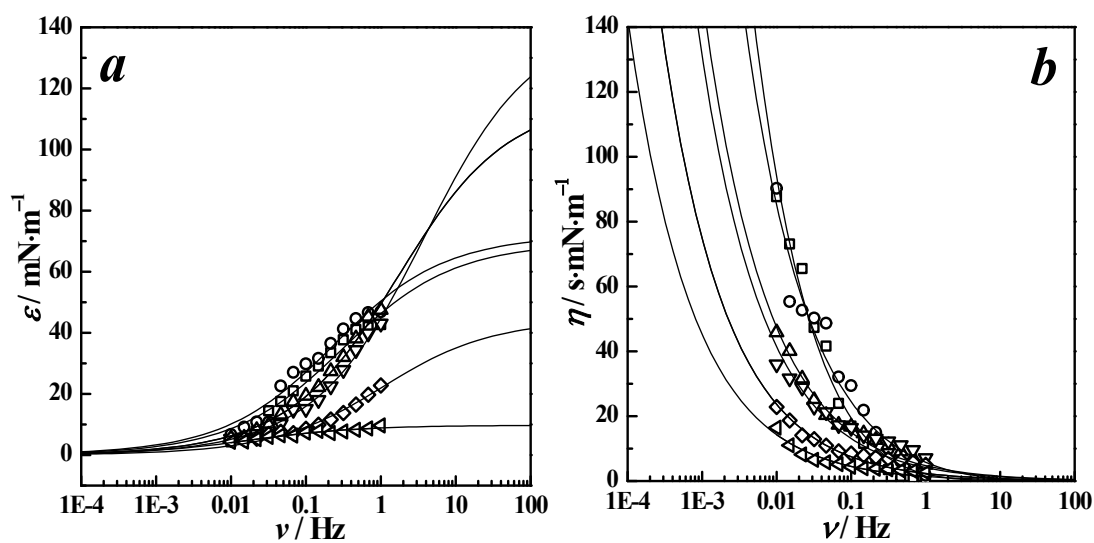


Fig.S12 Fitting results of dilational interfacial elasticity (ϵ , a) and interfacial viscosity (η , b) in

terms of LVT model for 12-2-12/0.3mMC₇OH aqueous solutions at 25°C. The symbols represent different surfactant concentrations: $\log(C/\text{mmol}\cdot\text{L}^{-1}) = -1.30$ (\square), -1.18 (\circ), -0.93 (\triangle), -0.74 (∇), -0.52 (\diamond), -0.30 (\blacktriangleleft)

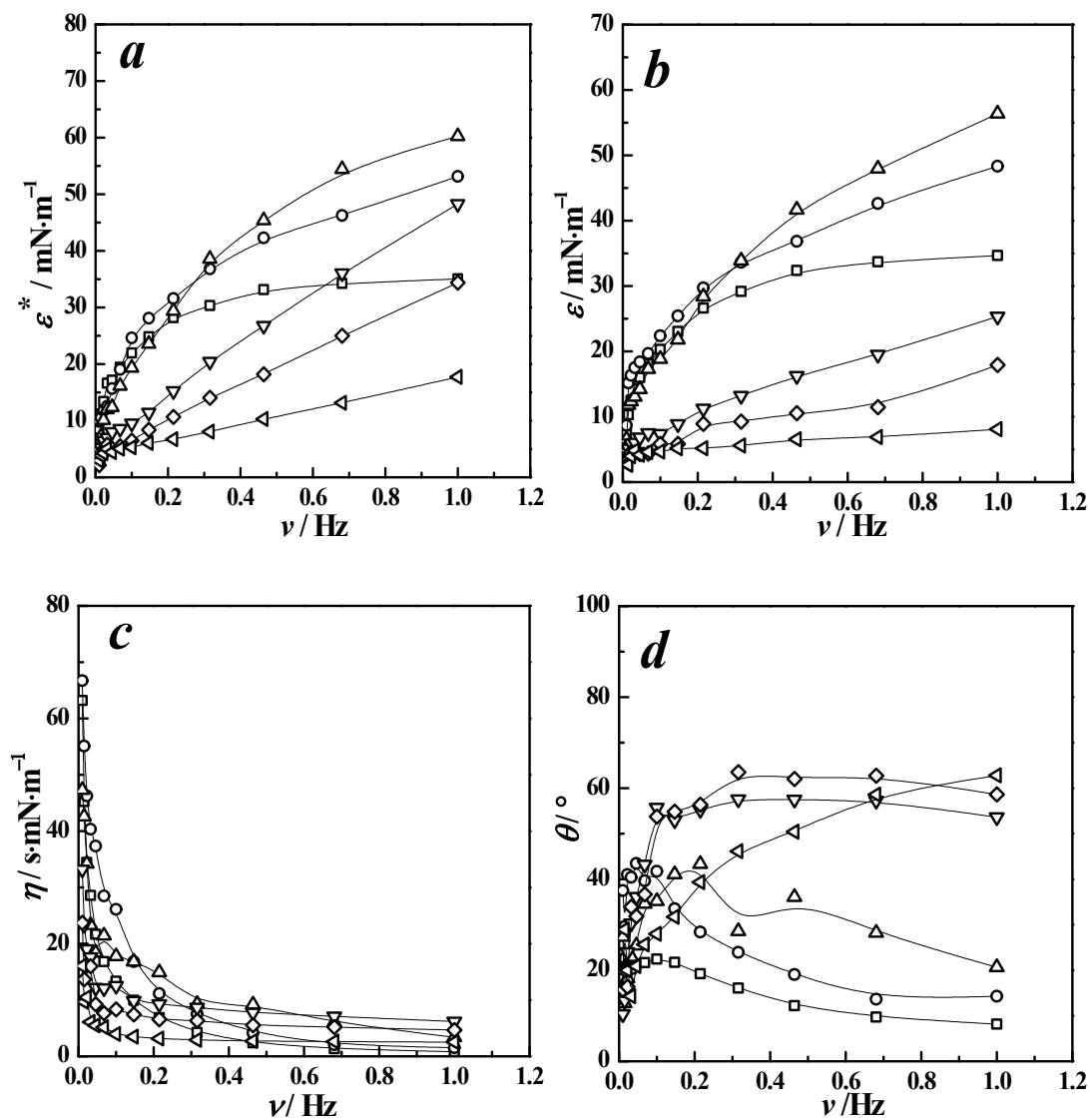


Fig.S13 The experimental plots of complex modulus (ϵ^* , *a*), interfacial elasticity (ϵ , *b*), interfacial viscosity (η , *c*) and phase angle (θ , *d*), as a function of frequency (ν), respectively, in 12-2-12/2mMC₇OH aqueous solutions at 25°C. The symbols represent different surfactant concentrations: $\log(C/\text{mmol}\cdot\text{L}^{-1}) = -1.38$ (\square), -1.18 (\circ), -0.93 (\triangle), -0.63 (∇), -0.52 (\diamond), -0.30 (\blacktriangleleft)

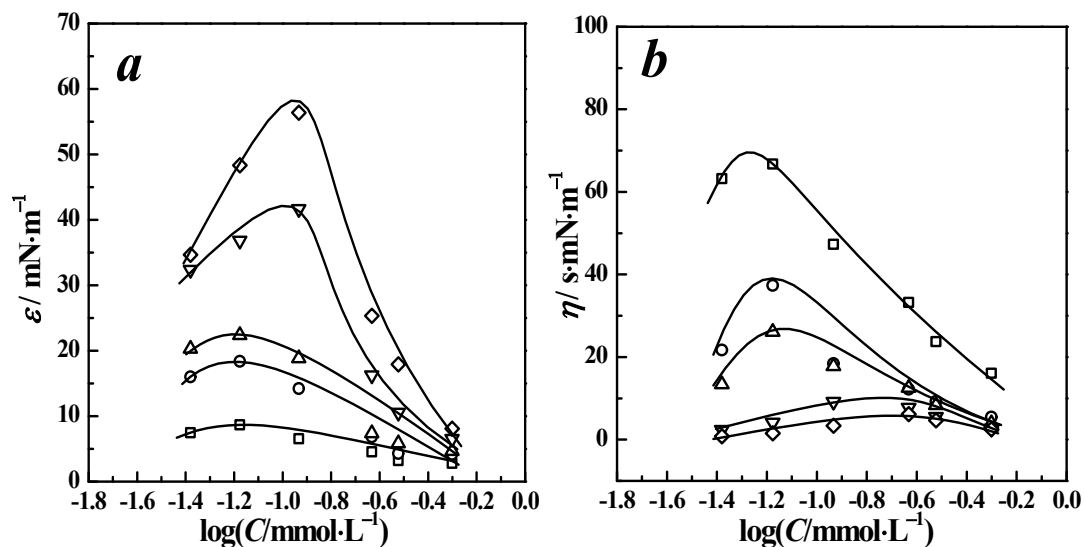


Fig.S14 Semilogarithmic plots of dilational interfacial elasticity (ϵ , *a*) and interfacial viscosity (η , *b*) of 12-2-12/2mMC₇OH as a function of the surfactant concentration C for different frequencies. The symbols represent $\nu/\text{Hz} = 0.01$ (\square), 0.046 (\circ), 0.1 (\triangle), 0.464 (∇) and 1 (\diamond)

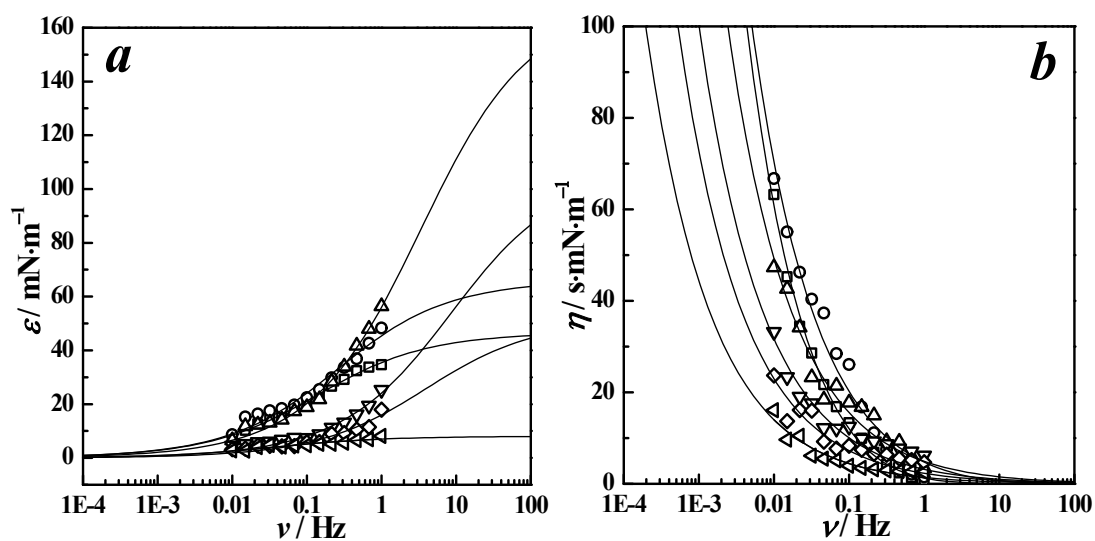


Fig.S15 Fitting results of dilational interfacial elasticity (ϵ , *a*) and interfacial viscosity (η , *b*) in terms of LVT model for 12-2-12/2mMC₇OH aqueous solutions at 25°C. The symbols represent different surfactant concentrations: $\log(C/\text{mmol}\cdot\text{L}^{-1}) = -1.38$ (\square), -1.18 (\circ), -0.93 (\triangle), -0.63 (∇), -0.52 (\diamond), -0.30 (\blacktriangleleft)

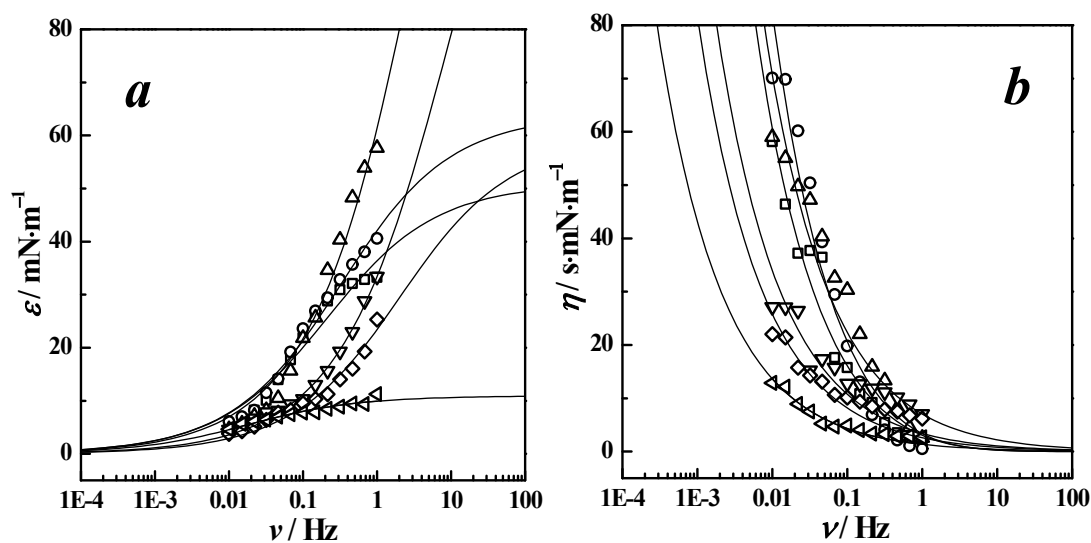


Fig.S16 Fitting results of dilational interfacial elasticity (ε , **a**) and interfacial viscosity (η , **b**) in terms of LVT model for 12-2-12/0.7 mmol·L⁻¹C₇OH aqueous solutions. The symbols represent different surfactant concentrations: $\log(C/\text{mmol}\cdot\text{L}^{-1}) = -1.38$ (\square), -1.18 (\circ), -0.93 (\triangle), -0.63 (∇), -0.52 (\diamond), -0.30 (\blacktriangleleft)

Table S2 Foam decay time $t_{1/2}^{\max}$ and limiting interfacial elasticity $\varepsilon_{0,fit}$ of 12-2-12/0.3mMC₇OH、12-2-12/0.7mMC₇OH and 12-2-12/2mMC₇OH mixed systems at the surface excess of 80%

system	12-2-12/0.3mMC ₇ OH	12-2-12/0.7mMC ₇ OH	12-2-12/2mMC ₇ OH
$10^{10}\Gamma_{\max}$ mol·cm ⁻²	3.62	3.92	3.41
80%* $10^{10}\Gamma_{\max}$ /mol·cm ⁻²	2.90	3.14	2.73
$C/\text{mmol}\cdot\text{L}^{-1}$	0.045	0.033	0.026
$\varepsilon_{0,fit}/\text{mN}\cdot\text{m}^{-1}$	54.82	81.92	60.13
$t_{1/2}^{\max}$ /min	846	1497	1102

Table S3 Fitting parameters $\varepsilon_{0,\text{fit}}$ and $\omega_{0,\text{fit}}$ of 12-2-12 and alcohol mixtures

12-2-12 + alcohol								
4.0 mmol·L ⁻¹ C ₆ OH			5.5 mmol·L ⁻¹ C ₆ OH			8.0 mmol·L ⁻¹ C ₆ OH		
<i>C</i>	$\varepsilon_{0,\text{fit}}$	$\omega_{0,\text{fit}}$	<i>C</i>	$\varepsilon_{0,\text{fit}}$	$\omega_{0,\text{fit}}$	<i>C</i>	$\varepsilon_{0,\text{fit}}$	$\omega_{0,\text{fit}}$
0.04	22	0.16	0.04	44	1.82	0.04	41	2.02
0.07	71	1.54	0.07	108	6.97	0.10	98	0.63
0.10	111	5.20	0.10	182	7.21	0.17	197	11.15
0.17	171	9.00	0.17	241	9.69	0.25	146	8.19
0.25	114	4.21	0.25	169	2.31	0.40	56	3.59
0.40	46	1.36	0.40	71	1.21	0.63	11	0.11
			0.63	12	0.55			
0.3 mmol·L ⁻¹ C ₇ OH			0.7 mmol·L ⁻¹ C ₇ OH			2.0 mmol·L ⁻¹ C ₇ OH		
0.05	58	0.67	0.04	51	0.81	0.04	47	0.86
0.07	72	1.49	0.07	64	6.32	0.07	66	1.63
0.12	117	10.74	0.12	206	8.51	0.12	170	11.19
0.18	143	14.23	0.23	155	16.94	0.23	107	3.94
0.30	45	6.59	0.30	80	5.06	0.3	52	4.92
0.50	10	0.11	0.50	11	2.64	0.5	8	0.24

Note: *C*, $\varepsilon_{0,\text{fit}}$ and $\omega_{0,\text{fit}}$ are in mmol·L⁻¹, mN·m⁻¹ and s⁻¹, respectively.